Carbohydrate Polymer Technologies and Applications 2 (2021) 100168

Contents lists available at ScienceDirect

Carbohydrate Polymer Technologies and Applications

journal homepage: www.sciencedirect.com/journal/carbohydrate-polymer-technologies-and-applications

Flow behavior and syneresis of ball milled rice starch and their correlations with starch structure

Luciana C. González [a,b], Maria A. Loubes [a,b], María M. Bertotto [c], Rosa I. Baeza [d], Marcela P. Tolaba [a,b,*]

[a] University of Buenos Aires, School of Exact and Natural Sciences, Department of Industries, Buenos Aires, Argentina
[b] CONICET-University of Buenos Aires Institute of Food Technology and Chemical Processes (ITAPROQ). Buenos Aires, Argentina
[c] Servicio Nacional de Sanidad y Calidad Agroalimentaria, Dirección General de Laboratorio Animal, Argentina
[d] Pontificia Universidad Católica Argentina, Facultad de Ingeniería y Ciencias Agrarias, Buenos Aires, Argentina

ARTICLE INFO

Keywords:
Ball milling
Rice starch
Pseudoplastic behavior
Viscosity
Starch structure
FT-IR spectroscopy

ABSTRACT

The effects of milling energy (0.26–4.08 kJ/g) on starch structure, flow behavior and syneresis of starch dispersions (4–8% w/v) were investigated. Crystallinity loss of starch (XRD analysis) during milling could be mathematically related with the increase of 1047 cm^{-1}/1022 cm^{-1} FT-IR intensity ratio (Ri) and it was also reflected by the changes in the shape and surface roughness of starch granules (SEM micrographs). Starch dispersions showed a Newtonian or pseudoplastic flow pattern dependent on starch concentration and milling energy. Consistency of starch dispersions (4 and 6%) remained constant during refrigerated storage only for severely milled starch. Syneresis diminished with increasing milling energy and starch concentration; it could be minimized (4% and 4.08 kJ/g) or completely eliminated (8% and 1.04 kJ/g). Significant correlations of Ri with consistency index and syneresis were found. Ball milling notably improved the suitability of starch as an ingredient in fluid or viscous foodstuffs.

1. Introduction

Starch is widely used in the food industry as a thickening or gelling agent. Particularly, the functional properties of rice starch are highly appreciated (Ashwar, Gani, Gani, Shah & Masoodi, 2018; Loubes, Barrera & Tolaba, 2016; Ye et al., 2016). It can be used as texturizing agent to improve product viscosity, syneresis control and shelf-life characteristics. Furthermore, thanks to its small granule size (3–8 μm), similar to that of fat globules, it is a convenient fat substitute.

Functional properties of starch are dependent on starch structure, which can be modified by chemical, physical and enzymatic methods (Jin, Li & Malaki Nik, 2018). The physical methods have received the attention of researchers, due to their simplicity, low cost and contribution to food safety because of the absence of chemical or biological agents (Ashogbon & Akintayo, 2014). In particular, ball milling is presented as a physical technology applied to cereals and their derivatives by means of wet and dry milling on a laboratory scale (Bindar, Efan & Rahmi, 2013; González, Loubes & Tolaba, 2018; He et al., 2014; Loubes & Tolaba, 2014). Recently, the use of the planetary ball mill to isolate rice and amaranth starch by wet milling in alkaline medium from whole grains has been successfully studied. The ability to work at high energies and the high degree of disaggregation allowed starch recoveries of 62–74% for rice and 47–57% for amaranth (Loubes et al., 2016; Roa Acosta, Solanilla Duque, Agudelo Laverde, Villada Castillo & Tolaba, 2020).

The degree of modification given by the planetary ball mill depends both on the intensity of the process and the nature of the starch, and is associated with the distortion of the ordered structure and the increase in the amorphous phase (Tan et al., 2015). Some researchers have shown that the modification conferred by the planetary mill can reach not only strictly crystalline regions but also double helix structures, located in less ordered areas (Liu, Ma, Yu, Shi & Xue, 2011). The ultra-fine pulverization reduces the starch granule size, the crystallinity of amylopectin molecules and their double helix conformation. Fragmentation of amylopectin increases the swelling capacity of starch granule favoring the starch gelatinization, the decrease of gelatinization enthalpy and onset gelatinization temperature (Alcázar-Alay & Meireles, 2015). Fourier transform infrared spectroscopy (FT-IR) has been widely used to

* Corresponding author at: Facultad de Ciencias Exactas y Naturales, Universidad de Buenos Aires, Intendente Güiraldes 2160 - Ciudad Universitaria, C1428EGA, Ciudad Autónoma de Buenos Aires, Argentina.
E-mail address: mtolaba@di.fcen.uba.ar (M.P. Tolaba).

https://doi.org/10.1016/j.carpta.2021.100168
Received 29 April 2021; Received in revised form 15 September 2021; Accepted 30 September 2021
Available online 9 October 2021

determine the composition of products and the chemical modifications induced by different food processing methods. FT-IR and XRD were used to evaluate the changes in the crystalline / amorphous fractions of corn (Liu et al., 2011), amaranth (Roa, Santagapita, Buera & Tolaba, 2014) and rice (Devi, Fibrianto, Torley & Bhandari, 2009) starches, subjected to high energy grinding.

Structural modifications such as changes in the particle size distribution and increased starch damage, resulting from the milling process, are reflected by changes in the hydration and paste properties of the starch suspensions (Barrera et al., 2013; Chiang & Yeh, 2002; Hossen et al., 2011; Zhang, Zhao & Xiong, 2010). These starch modifications are required for liquid food development as well as for formulation of dressing or cream soup (Roa, Baeza & Tolaba, 2015). Frequently, viscometers and rheometers are used to simulate food processing and to determine flow and pasting behavior of starch dispersions. Related works reported in the literature show a constant interest in investigating the behavior of starch during food processing, as well as the aptitude of starch as a functional ingredient in different food products (Alcázar-Alay & Meireles, 2015; Ashwar et al., 2018; Wani et al., 2012).

Although starch functional properties have widely been correlated with starch structure, so far, no attempt has been made to correlate flow properties of physically modified rice starch with its FT-IR structural feature.

The objectives of the present study were: (i) to study the effect of milling energy on changes in the starch structure and its correlation with functional properties; (ii) to determine the effects of starch concentration and milling energy level on flow behavior; (iii) to investigate the syneresis and stability of rice starch dispersions during 48 h of refrigerated storage. In addition, the morphological change in starch was qualitatively described based on SEM images.

2. Materials and methods

2.1. Material

Native rice starch of food grade (Remy B7, BeneoGmbH, Germany) was supplied by Saporiti S.A. (Buenos Aires, Argentina). The amylose content of the rice starch was 18.4 g/100 g of total starch, determined according to an iodine binding-based method of Li, Wang and Zhu (2016). Chemical composition (dry basis) of rice starch was provided by the manufacturer as follows: 88.7% carbohydrates (by difference), 13.7% moisture, 1.0% protein, 0.0% lipid, 0.2% ash.

2.2. Rice starch modification by ball milling

Starch was ground in a planetary ball mill model PM 100 manufactured by Retsch (Retsch GmbH, Germany) with zirconium jar (500 mL) and balls (diameter: 5 mm) at different levels of milling energy within the range 0.26–4.08 kJ/g (equivalent to 5.3–87.1 min of milling time) and constant rotational speed of 400 rpm. A previous calibration was made by using an empty jar (energy at "ralentí") to obtain the energy delivered to the jar's content (starch sample and balls). Starch sample (115 g) was used in a starch:balls mass ratio of 1:5 according to method of Gonzalez et al. (2018) which involved pauses of 40 min each 10 min of grinding and a change in the rotational direction of the jar every 30 s. By this method, sample temperature was controlled and it never exceeded 55 °C. After grinding, a manual sieving was carried out through a Zonytest (Rey & Ronzoni, Buenos Aires, Argentina) sieve (No. 6: 3360 μm) to separate the starch from the grinding balls. The grinding elements (jug and balls) and the sieve were carefully washed and brushed with a detergent cleaning solution and rinsed with plenty of water. Finally, they were rinsed twice with distilled water and allowed to dry. Native rice starch was set as control sample.

2.3. FT-IR measurements

FT-IR spectra of native and modified starches were obtained in a FT-IR spectrometer Nicolet iN10 (Thermo Scientific, EE. UU.) with a mercury-cadmium telluride detector (MCT, Thermo Scientific), cooled with liquid nitrogen. Each spectrum represents the average of 64 scans at 25 °C with a resolution of 4 cm^{-1} acquired between 600 and 4000 cm^{-1}. A background spectrum was previously recorder in air (without sample). Spectral analysis, based on absorbance curves, was performed using OriginPro 8.5 software (OriginLab Corp, Northampton, USA). First, the baseline was corrected, then the curves were normalized (between 0 and 1) for figure presentation and finally, the peaks of interest and their respective intensities were identified. The intensity ratio (Ri) corresponding to 1047/1022 cm^{-1} was conveniently used to characterize the starch structure (Yang et al., 2019).

2.4. XRD analysis

XRD analysis was performed using a Philips diffractometer model X'Pert MPD (PANalytical B.V., Netherlands) under Kα-radiation of copper ($\lambda = 0.154$ nm). The scanning region of the diffraction angle (2θ) was 6–32° and the scanning speed was set at 0.9°/min. The spectral analysis and the quantification of crystallinity degree were carried out according to the method previously described in González et al. (2018).

2.5. Scanning electron microscopy (SEM)

Rice starch samples were fixed on a circular aluminum stub with double-sided sticky tape, sputter coated with gold and examined and photographed in a FESEM-Carl Zeiss Model Supra 40 field emission scanning electron micro scope (Carl Zeiss, Oberkochen, Germany) coupled with energy-dispersive X-ray detector (EDX) at an accelerating voltage of 3 kV. The images were recorded at room temperature, with magnification level from 3000x to 25000x, a qualitative visual analysis was then performed. The procedure described by Darchuk et al. (2010) was adopted in order to achieve the elemental composition of starch sample by means of the SEM/EDX analysis.

2.6. Flow properties of starch dispersions

Starch dispersions were prepared at 4, 6 and 8% w/v in distilled water. The percentage range selected represents starch concentrations in food from a beverage to a dressing or cream soup. The mixing procedure involved 30 min of stirring at 25 °C, followed by 15 min of heating at 95 °C in a thermostatic bath and finally cooling to 25 °C. Flow properties of starch dispersions were determined immediately (0 h) and 48 h after of storage at 4° C using a rotational viscometer (Brookfield DV- LVT; Brookfield Engineering Laboratories, Inc., Middleboro, U.S.A) with coaxial cylinder probes. The measurement method of Roa et al. (2015) was adopted with some modifications. Tests were performed at 25 °C using several rotational speeds corresponding to a percentage torque ranging from 10 to 100%. For the different systems, different accessories and spindles were used according to the range of viscosity and maximum torque (UL / Y adapter with UL spindle or Small sample adapter with cylindrical probes). Rheological tests were duplicated and the data obtained were fitted to the power law:

$$\sigma = K\gamma^{n} \quad (1)$$

Where σ is the shear stress (Pa) and $\dot{\gamma}$ is the shear rate (s^{-1}). The rheological parameters determined were the consistency index (K; Pa s^{n}) and the flow behavior index (n; dimensionless). The effect of refrigerated storage on rheological parameters was investigated.

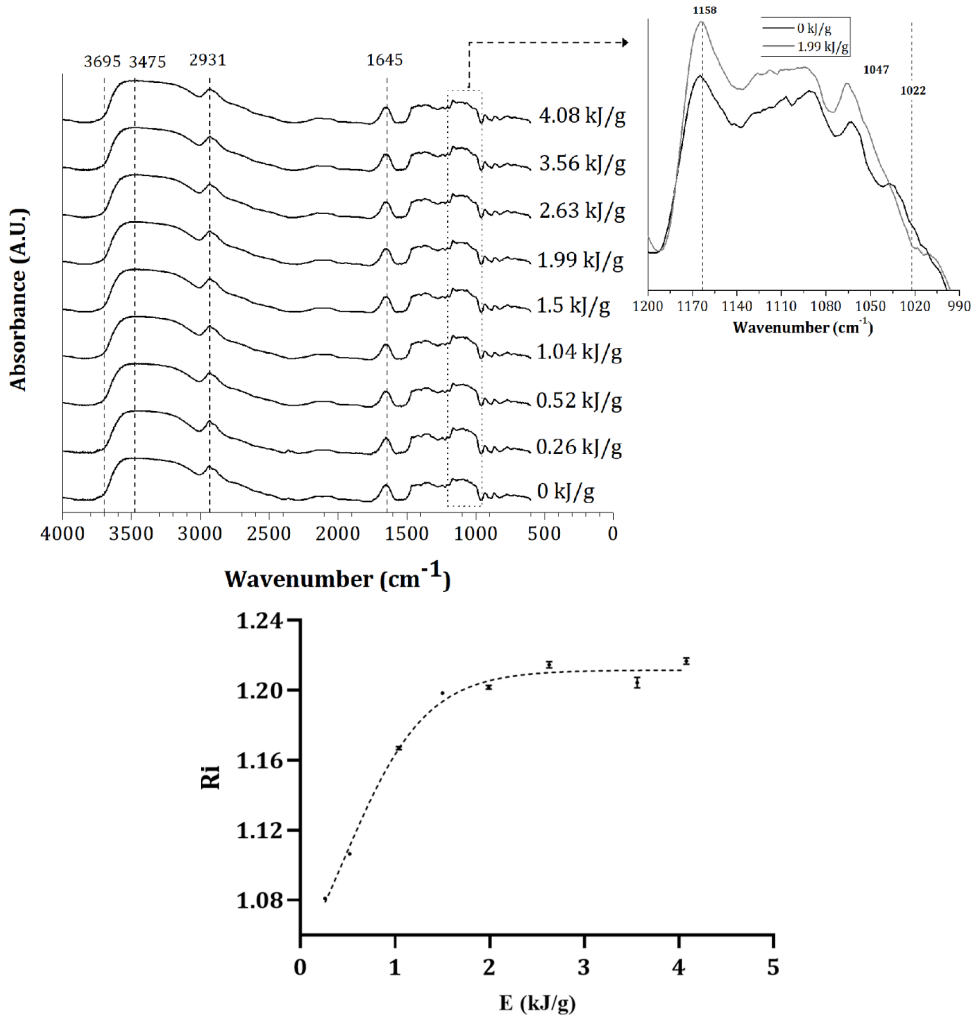

Fig. 1. FT-IR analysis. (a) FT-IR spectra of rice starches treated with high energy milling (0.26 to 4.08 kJ/g) and native starch (control sample), (b) Ratio of intensities (Ri: 1047 cm^{-1}/1022 cm^{-1}) of rice starches as a function of milling energy (E).

2.7. Syneresis

Starch (20 g) dispersions at 4 and 8% (w/w, dry basis) were prepared in 50 ml centrifuge tubes. According to the method of Loubes (2015), the starch dispersion was homogenized for 10 s in a AV11 vortex mixer (Decalab S.R.L., Buenos Aires, Argentina), heated in a shaking water bath at 95 °C for 15 min and stored at 4 °C for 48 h. After storage, the sample was shaken and centrifuged at 700 × g in a Rolco 2070 centrifuge (Rolco S.R.L., Buenos Aires, Argentina) for 10 min. The tests were performed in triplicate. The amounts of gel (before centrifugation) and water exudate were determined gravimetrically and the percentage of syneresis was calculated as follows:

$$Syneresis(\%) = \left(\frac{supernatant\ mass}{gel\ mass}\right).100 \quad (2)$$

2.8. Statistical anaShlysis

Analysis of variance (ANOVA), and regression and correlation analyses were performed using the statistical program Statgraphics Centurion version XVI (Statistical graphics Corporation, USA). A confidence level of 95% was used except in the case of Pearsonś correlation coefficients, which were obtained with a confidence level of 99%.

3. Results and discussion

3.1. FT-IR analysis of rice starches

The FT-IR spectra of native rice starch (0 kJ/g) and of rice starches treated at different levels of milling energy (0.26–4.08 kJ/g) are shown in Fig. 1a.

Native and modified rice starches exhibited similar patterns, characterized by an absorption band in the range of 3475–3695 cm^{-1} and a peak at 2931 cm^{-1}, corresponding to the stretching vibrations O–H and C–H, respectively, and a signal at 1158 cm^{-1} in the fingerprint region which was caused by the bending and asymmetric stretching of the C–O–C glycosidic bond (Sha et al., 2012). The infrared spectra also presented a peak at 1645 cm^{-1}, this is due to the bound water present in the starch (Ashwar et al., 2018). No new peaks were observed in relation to native starch; therefore, it can be inferred that milling treatment did not create new functional groups. The analysis of the FT-IR spectra in the range of 1000–1050 cm^{-1} was used based on literature reports for potato starch (Capron, Robert, Colonna, Brogly & Planchot, 2007), maize starch (Liu et al., 2011) and amaranth starch (Roa et al., 2014a,Roa, Santagapita, Buera & Tolaba, 2014). Although there are no “peaks” in this range, the variations in the intensities at 1047 cm^{-1} and 1022 cm^{-1} have been attributed to the C–O–H bending modes and are associated with the crystalline to amorphous transitions (Capron et al., 2007). Therefore, the changes in the 1047cm^{-1}/1022 cm^{-1} intensity ratio (Ri)

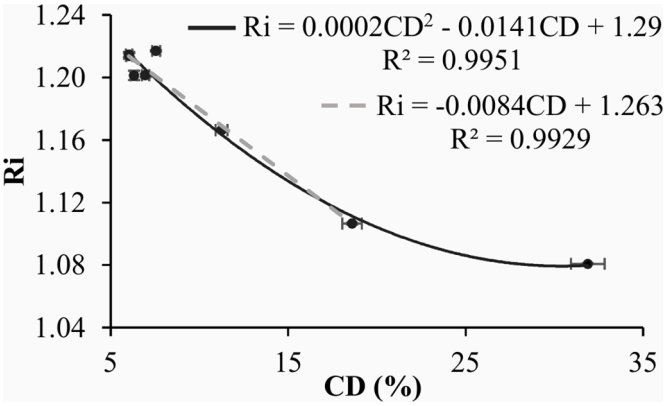

Fig. 2. Relationships between FT-IR intensity ratio (Ri) and crystallinity degree (CD) by XRD analysis. The values represent the average value from five (Ri) or three (CD) determinations ± standard deviation.

was adopted to follow the crystallinity loss during milling.

Fig. 1b shows the effect of the milling energy (0.26–4.08 kJ/g) on the Ri values. The experimental data were satisfactorily fitted ($R^2 = 0.992$) to a dose-response sigmoid nonlinear regression model:

$$Ri = 1 + \left(\frac{0.212}{1 + 10^{0.4899-E}}\right).100 \quad (3)$$

The increase in grinding energy caused a significant increase in Ri, from 1.08 to 1.2 between 0.26 kJ/g and 1.5 kJ/g; however, when the energy was higher than 1.5 kJ/g the change was not remarkable (Ri = 1.2 - 1.22). In turn, native starch presented a Ri value of 1.09, similar to that of starch subjected to 0.26 kJ/g of milling energy (Ri = 1.08). Liu et al. (2011) obtained a complete resolution of the 1047 cm^{-1} peak, corresponding to the total amorphization of corn starch structure, after 2 h of continuous ball milling at low temperature. In contrast to the present work, Devi et al. (2009) achieved an increase in Ri from 1.55 to 1.79 and a complete amorphization when grinding rice starch for 60 min by cryo-milling.

As previously reported (González et al., 2018), the degree of crystallinity of rice starch measured by XRD progressively decreased with increasing milling energy (XRD data in Supplementary Figure). Those results allow corroborating the data obtained by FT-IR and its concordance with the increase in Ri values. A second order polynomial nonlinear relationship ($R^2 > 0.99$) could be established between Ri and crystallinity degree (CD) obtained by XRD analysis. In addition, for CD values below 20% the variables were found to be linearly related (Fig. 2).

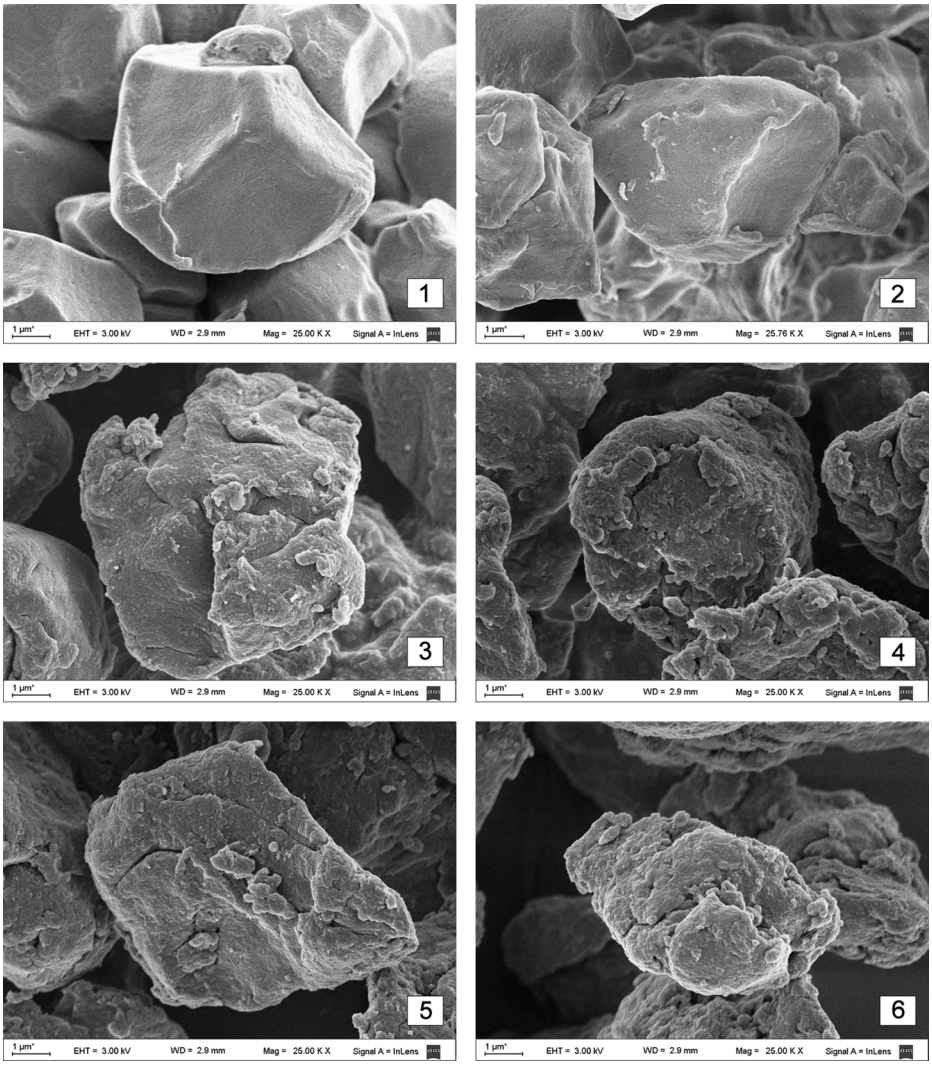

Fig. 3. SEM images of modified rice starches and control sample (native starch) with magnification of 25,0 kx as function of milling energy (1: 0.0 kJ/g; 2: 0.26 kJ/g; 3: 1.5 kJ/g; 4: 1.99 kJ/g; 5: 2.63 kJ/g; 6: 4.08 kJ/g).

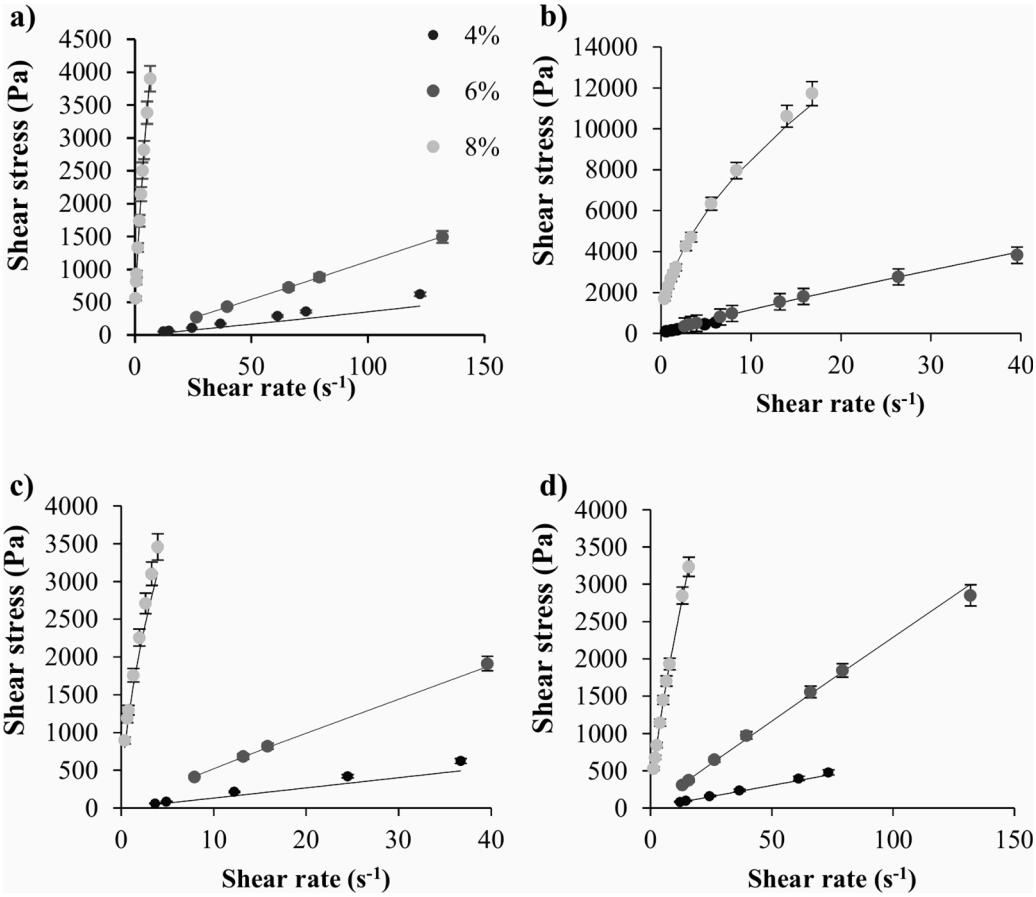

Fig. 4. Relationship between shear stress and shear rate as function of starch concentration and milling energy for 0 h of storage time. (a) 0 kJ/g (control), (b) 1.04 kJ/g, (c) 1.99 kJ/g, d) 4.08 kJ/g. The values represent the average value from two determinations ± standard deviation.

It was reported that decreasing the crystalline order in starch granules leads to irreversible changes in the functional properties such us granule swelling, pasting and solubility capacity (Roa et al., 2014a; Singh, Singh, Kaur, Singh Sodhi & Singh Gill, 2003). The corresponding increase in the proportion of the amorphous phase promotes the entry of water to the granules and its interaction with the polymer chains, favoring the water solubility and swelling capacity of the starch (González et al., 2018).

3.2. SEM analysis of modified starches

Native rice starch granules presented polyhedral shape with defined edges and smooth surface, without visible cracks or pores. Starch granules subjected to the lowest milling treatment (0.26 kJ/g, Figs. 2,3) showed slight surface roughness. At moderate milling treatments (milling energy between 0.52 and 1.5 kJ/g) small starch fragments separated from the granules and signs of mechanical damage were observed (Fig. 3) due to compression and impact forces acting on the starch granules during grinding process.

At energies above 1.99 kJ/g (Figs. 3–5) the presence of cracks on the surface became noticeable along with the increase in the amount of detached small particles. The starch granules subjected to severe milling conditions (4.08 kJ/g) showed undefined shape and a completely rough surface; in turn, the polyhedral shape characteristic of native starch was fully disappeared.

Other authors (Chen, Lii & Lu, 2003; Dai, Li, Zhang & Cheng, 2018; He et al., 2014) also analyzed ball milled starches by SEM micrography and noticed that starch granules lost flatness and smoothness, and became rough with the formation of some grooves as milling time advanced.

SEM/EDX analysis was performed to confirm the absence of zirconium. The microanalysis of the starch sample for the most severe milling condition (4.08 kJ/g) revealed the presence of carbon and oxygen but zirconium was not detected (Supplementary file).

3.3. Flow behavior of starch dispersions

Fig. 4 shows the significant effect of milling energy and starch concentration on flow curves for 0 h of storage time. The plotted points correspond to values between 10 and 100% of the maximum torque for the different spindles used. The most concentrated sample (8%) stands out for its marked pseudoplastic character. At each concentration, a significant increase in shear stress (τ) was observed in the modified starch samples at 1.04 kJ/g (Fig. 4b) in comparison with control sample (Fig. 4a). However, as the grinding energy increased (Fig. 4c and d) the values of τ decreased and the differences between 4 and 6% were more notable. Flow curves for 48 h of storage time are presented as Supplementary Figure.

Flow behavior was fitted by means of power law model. The consistency coefficient K and flow index n, are shown in Table 1 for starch dispersions at 0 h and 48 h of refrigerated storage. The Eq. (1) provided a satisfactory fit ($R^2 > 0.98$) both before and after storage.

All modified rice starches presented higher K values than that of the control sample. Values of n index evidenced the pseudoplastic character ($n < 1$) of the starch dispersions. The viscosity is determined by both particle volume fraction and rigidity. In a dilute system, the viscosity is proportional to the volume fraction of the swollen particles, which depends on the swelling capacity; whereas in concentrated systems (closely packed systems) the rigidity of the particles is the decisive factor (Steeneken, 1989).

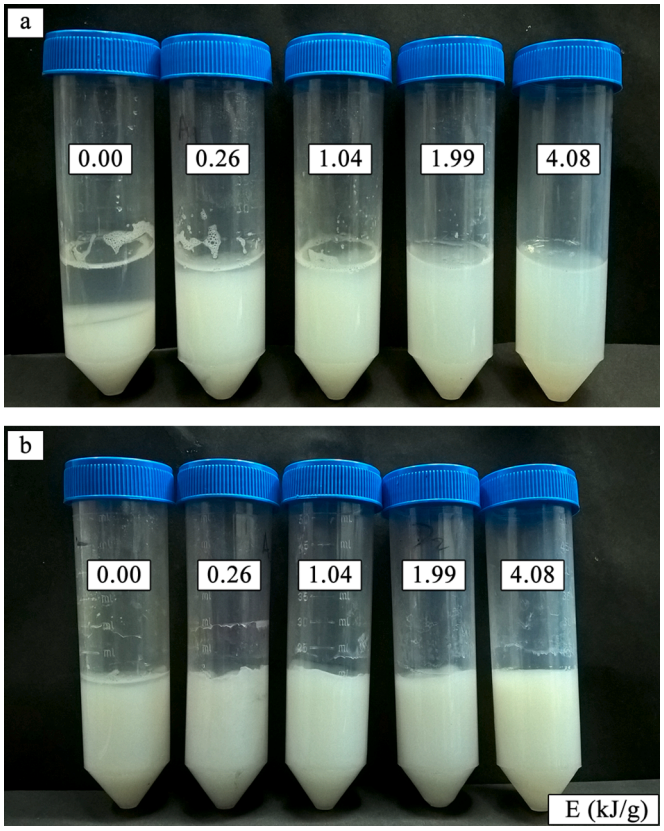

Fig. 5. Photographs of starch gels syneresis as function of milling energy (E, kJ/g) and starch concentration: (a) 4%, (b) 8%.

The *K* coefficient increased exponentially with starch concentration at a fixed level of milling energy. In agreement with the present work, Roa et al. (2015) also observed an increment in K values with increasing flour concentration (from 4 to 8%) when they studied the rheological behavior of modified amaranth flour obtained by ball milling. The consistency increase can be associated with the formation of a molecular network of amylose and amylopectin molecules, induced by thermo-mechanical activation in the ball mill (Autio & Eliasson, 2009).

At 1.04 kJ/g and a fixed concentration value (4, 6 or 8% at 0 h and 4 or 6% at 48 h), *K* reached the maximum value. The pseudoplastic character is most evident between 0 and 1.04 kJ/g particularly for the 8% starch dispersion.

Above 1.04 kJ/g a reduction of *K* values was observed as pulverization degree increased, which was in concordance with the rise of the amorphous phase (Ri) determined by FT-IR. Particularly for milling energy within 1.04–4.08 kJ/g, a significant correlation between consistency and Ri was found (*K*-Ri: $r > 0.98$, $p < 0.01$). The reduction of K values by increasing milling severity can be attributed to the breakdown of the starch granules and the increase of the amorphous phase according to Roa et al. (2015).

The effect of grinding energy on *K* and *n* values was very significant mainly for starch concentration of 8%. High impact ball milling produces changes in the starch structure also affecting starch solubility, hydration and swelling properties among other functional attributes González et al. (2018).

For 4% and 6% starch dispersions, storage produced a general decrease in the consistency index while it caused the opposite effect in the 8% dispersions. The formation of a strong gel was observed in the case of 8% starch dispersions treated at low milling energy (see Supplementary Figure), while from 1.04 kJ/g the systems remained fluid, retaining a high consistency despite storage. After refrigerated storage, an increase in the value of *n* was observed in the 4% and 6% dispersions showing a reduction in their pseudoplastic character. In contrast, the more concentrated samples (8%) milled between 0–1.04 kJ/g presented lower flow indexes, which could be associated with the gelation of this system during storage.

It should be noted that the highest stability (measured in terms of the consistency index) was obtained for the 4% and 6% starch dispersions using the highest energy level (4.08 kJ/g). This result is relevant as it broadens the applications of starch by controlling the degree of

Table 1
Consistency (*K*) and flow (*n*) indexes for rice starch dispersions at 25 °C as function of milling energy, starch concentration and storage time.

Concentration (%)	Energy (kJ/g)	*N*	*K* (Pa*s^n)	*N*	*K* (Pa*s^n)
		0 h	0 h	48 h	48 h
4	0	1.06 ± 0.09^{a}	3.76 ± 0.13^{m}	1.10 ± 0.07^{b}	2.26 ± 0.12^{m}
	0.26	0.98 ± 0.08^{a}	24.8 ± 0.61^{j}	1.03 ± 0.08^{b}	23.8 ± 1.0^{j}
	1.04	0.78 ± 0.05^{c}	127 ± 8 g	0.93 ± 0.06^{c}	27.8 ± 1.5^{i}
	1.99	0.99 ± 0.09^{a}	17.4 ± 1.1^{k}	1.00 ± 0.06^{b}	13.3 ± 0.5^{k}
	4.08	0.97 ± 0.04^{a}	7.30 ± 0.78^{l}	0.99 ± 0.05^{b}	6.32 ± 0.14^{l}
6	0	1.05 ± 0.07^{a}	8.83 ± 0.76^{l}	1.35 ± 0.11^{a}	1.55 ± 0.02^{l}
	0.26	0.99 ± 0.09^{a}	45.7 ± 1.3^{i}	0.90 ± 0.08^{c}	57.7 ± 1.2 g
	1.04	0.89 ± 0.07^{b}	150 ± 18^{f}	0.91 ± 0.04^{c}	122 ± 9^{f}
	1.99	0.93 ± 0.03^{b}	62.1 ± 1.1^{h}	0.99 ± 0.07^{b}	37.0 ± 2.5^{h}
	4.08	0.97 ± 0.04^{a}	26.0 ± 1.3^{j}	0.89 ± 0.06^{c}	27.2 ± 1.7^{i}
8	0	0.69 ± 0.05^{c,d}	1083 ± 32^{c}	0.44 ± 0.00^{f}	5369 ± 137^{a}
	0.26	0.64 ± 0.05^{d}	2257 ± 84^{b}	0.41 ± 0.01 g	3855 ± 104^{b}
	1.04	0.53 ± 0.03^{e}	2538 ± 110^{a}	0.46 ± 0.01^{f}	2196 ± 99^{c}
	1.99	0.59 ± 0.03^{de}	1380 ± 56^{d}	0.58 ± 0.03^{e}	1423 ± 74^{d}
	4.08	0.74 ± 0.01^{c}	418 ± 14^{e}	0.83 ± 0.02^{d}	278 ± 11^{e}

Different letters in the same column indicate significant differences ($p < 0.05$). Mean and standard deviation values of duplicates are reported.

Table 2
Syneresis (%) of rice starch gels (4 and 8%) stored in refrigeration for 48 h, together with values of particle size distribution (D_{50}) and swelling power at 85 °C of rice starch as a function of milling energy. $E = 0$ kJ/g corresponds to native starch.

Energy (kJ/g)	Syneresis (%) 4%	Syneresis (%) 8%	D_{50} (μm)	Swelling Power (g/g)
0	47 ± 2^{a,1}	8 ± 1^{a,2}	61 ± 11^{b}	7.4 ± 0.1^{a}
0.26	18 ± 8^{b,1}	0.3 ± 0.3^{b,2}	16.9 ± 0.6^{a}	12.7 ± 0.5^{b}
1.04	7 ± 4^{c,1}	0.00 ± 0.00^{b,2}	13.4 ± 0.2^{a}	15.9 ± 0.4^{c}
1.99	2 ± 3^{d,1}	0.02 ± 0.03^{b,2}	12.2 ± 0.1^{a}	16.4 ± 0.7^{c,d}
4.08	0.10 ± 0.03^{e,1}	0.00 ± 0.00^{b,1}	13.2 ± 0.3^{a}	16.4 ± 0.6^{c,d}

The listed values represent the average value from three (syneresis and swelling power) or five (D_{50}) determinations ± standard deviation. The means in the columns with different letters in the superscript are significantly different from the grinding energy ($p < 0.05$). The means of syneresis in the rows with different numbers in the superscript are significantly different from the starch concentration ($p < 0.05$). D_{50}, swelling power: obtained from González et al. (2018).

modification during starch processing in the planetary ball mill.

3.4. Syneresis

Fig. 5 shows the physical changes in the rice starch gels after storage at 4 °C for 48 h. It was shown that the release of water depends not only on the level of modification of the starch in the planetary ball mill, but also on the concentration of starch in the gel.

For the concentrations tested (4 and 8%), all modified starches presented a lower percentage of syneresis with respect to the native starch (Table 2). For starch gels at 4% the syneresis decreased 99.8% from 47 ± 2% (for native starch) to 0.10 ± 0.0% (for modified starch at 4.08 kJ/g). Other physical modification methods of rice starch were found to reduce the percentage of syneresis of the gels: Ashwar et al. (2014) reduced the expulsion of water between 8.7 and 14.0% through the application of irradiation, while Ye et al. (2016) decreased it by 12.4% with the cooking-extrusion method. It should be noted that the comparison with literature data is difficult due to the variation in the methods for determining syneresis.

The syneresis levels in the present work (Table 2) were lower than those obtained by Ali, Wani, Wani and Masoodi (2016), who reported values from 79.2 to 81.0 ± 0.3% for rice starch gels at 2% after 48 h of storage. Mizrahi (2010) explains that increasing the concentration of the polymer constituting the gel allows to minimize syneresis since the higher the concentration of the polymer the osmotic pressure increases, encouraging water to enter the gel. If the osmotic pressure is lower, the pressure of the network to return to its initial state will exceed the osmotic pressure and syneresis will occur.

Furthermore, gels with a syneresis value of 0.3% after 48 h of refrigerated storage could be achieved when solutions of modified starch were prepared under the mildest condition (0.26 kJ/g) at a concentration of 8%.

A correlation was found ($r = -0.80$; $p < 0.01$) between syneresis values at 4% and the structural results obtained by FT-IR spectroscopy (Ri) from the correlation analysis (see Supplementary file). In addition, it can be appreciated in Table 2 that the expulsion of water from the modified starch gels was also related to previously published structural and functional parameters such as particle size distribution (D_{50}) and swelling power (SP) measured at 85 °C (González et al., 2018). An increase in particle size is associated with higher syneresis percentages (D_{50} - Syneresis; $r = 0.96$; $p < 0.01$) and a higher swelling power, related to water retention of the starch network, is reflected in lower syneresis values (SP - Syneresis; $r = -0.99$; $p < 0.01$). Since the application of native starches in liquid formulations is limited due to their high values of syneresis, the mechanical modification in planetary ball mill results an effective strategy to significantly reduce the syneresis of starch without the need to increase the concentration of starch in the dispersion.

4. Conclusions

High impact milling of rice starch resulted in altered structural and physicochemical properties. The planetary ball milling produced a reduction in the crystallinity degree and the consequent increase in the amorphous phase of starch granules. These structural changes brought about the pseudoplastic behavior of modified rice starches and the decreasing consistency coefficient once the 1.04 kJ/g level of milling energy was exceeded.

Although significant effects of starch concentration and milling energy on the flow behavior and the stability of the starch gels were found, the effect of concentration on consistency (exponential effect) and flow index (quadratic effect) prevailed for both 0 h and 48 h measurements. Higher viscosity, achieved with the highest modification levels for 8% starch dispersions, favored the stability of the gels during storage, avoiding syneresis. In summary, planetary ball milling is presented as an eco-friendly alternative to modify native rice starch properties. By selecting milling energy and starch concentration, different rheological properties can be obtained for specific applications in liquid or creamy systems of interest to the cosmetic, pharmaceutical, and food industries.

Declaration of Competing Interest

The authors declare that they have no known competing financial interests or personal relationships that could have appeared to influence the work reported in this paper.

Acknowledgments

The authors acknowledge the financial support from Agencia Nacional de Promoción Científica y Tecnológica, ANPCyT, (PICT 2018–01619), CONICET, and Universidad de Buenos Aires (UBACYT 20020170100367BA).

The authors declare that there is no conflict of interest regarding the publication of this article.

Supplementary materials

Supplementary material associated with this article can be found, in the online version, at doi:10.1016/j.carpta.2021.100168.

References

Alcázar-Alay, S. C., & Meireles, M. A. A. (2015). Physicochemical properties, modifications and applications of starches from different botanical sources. *Food Science and Technology, 35*, 215–236. https://doi.org/10.1590/1678-457X.6749

Ali, A., Wani, T. A., Wani, I. A., & Masoodi, F. A. (2016). Comparative study of the physico-chemical properties of rice and corn starches grown in Indian temperate climate. *Journal of the Saudi Society of Agricultural Sciences, 15*(1), 75–82. https://doi.org/10.1016/j.jssas.2014.04.002

Ashogbon, A. O., & Akintayo, E. T. (2014). Recent trend in the physical and chemical modification of starches from different botanical sources: A review. *Starch-Stärke, 66* (1–2), 41–57. https://doi.org/10.1002/star.201300106

Ashwar, B. A., Gani, A., Gani, A., Shah, A., & Masoodi, F. A. (2018). Production of RS4 from rice starch and its utilization as an encapsulating agent for targeted delivery of probiotics. *Food Chemistry, 239*, 287–294. https://doi.org/10.1016/j.foodchem.2017.06.110

Ashwar, B. A., Shah, A., Gani, A., Rather, S. A., Wani, S. M., Wani, I. A., et al. (2014). Effect of gamma irradiation on the physicochemical properties of alkali-extracted rice starch. *Radiation Physics and Chemistry, 99*, 37–44. https://doi.org/10.1016/j.radphyschem.2014.02.002

Autio, K., & Eliasson, A. C. (2009). Chapter 14-rye starch. In J. BeMiller, & R. Whistler (Eds.), *Starch (Third edition)* (pp. 579–587). San Diego: Academic Press.

Barrera, G. N., Bustos, M. C., Iturriaga, L., Flores, S. K., León, A. E., & Ribotta, P. D. (2013). Effect of damaged starch on the rheological properties of wheat starch suspensions. *Journal of Food Engineering, 116*(1), 233–239. https://doi.org/10.1016/j.jfoodeng.2012.11.020

Bindar, Y., Efan, A., & Rahmi. (2013). Sodium hydroxide (NaOH) concentration and steeping time duration effects on starch production from dry-milled low quality rice IR 64 grade 3 flour using alkaline-protease enzyme digestion method. *International Food Research Journal, 20*, 1353–1358.

Capron, I., Robert, P., Colonna, P., Brogly, M., & Planchot, V. (2007). Starch in rubbery and glassy states by FTIR spectroscopy. *Carbohydrate Polymers, 68*(2), 249–259. https://doi.org/10.1016/j.carbpol.2006.12.015

Chen, J. J., Lii, C. Y., & Lu, S. (2003). Physicochemical and morphological analyses on damaged rice starches. *Journal of Food and Drug Analysis, 11*(4), 283–289. https://doi.org/10.38212/2224-6614.2684

Chiang, P. Y., & Yeh, A. I. (2002). Effect of soaking on wet-milling of rice. *Journal of Cereal Science, 35*(1), 85–94. https://doi.org/10.1006/jcrs.2001.0419

Dai, L., Li, C., Zhang, J., & Cheng, F. (2018). Preparation and characterization of starch nanocrystals combining ball milling with acid hydrolysis. *Carbohydrate Polymers, 180*, 122–127. https://doi.org/10.1016/j.carbpol.2017.10.015

Darchuk, L., Tsybrii, Z., Worobiec, A., Vázquez, C., Palacios, O. M., Stefaniak, E. A., et al. (2010). Argentinean prehistoric pigments' study by combined SEM/EDX and molecular spectroscopy. *Spectrochimica Acta Part A: Molecular and Biomolecular Spectroscopy, 75*(5), 1398–1402.

Devi, A. F., Fibrianto, K., Torley, P. J., & Bhandari, B. (2009). Physical properties of cryomilled rice starch. *Journal of Cereal Science, 49*(2), 278–284. https://doi.org/10.1016/j.jcs.2008.11.005

González, L. C., Loubes, M. A., & Tolaba, M. P. (2018). Incidence of milling energy on dry-milling attributes of rice starch modified by planetary ball milling. *Food Hydrocolloids, 82*, 155–163. https://doi.org/10.1016/j.foodhyd.2018.03.051

He, S., Qin, Y., Walid, E., Li, L., Cui, J., & Ma, Y. (2014). Effect of ball-milling on the physicochemical properties of maize starch. *Biotechnology Reports, 3*, 54–59. https://doi.org/10.1016/j.btre.2014.06.004

Hossen, M. S., Sotome, I., Takenaka, M., Isobe, S., Nakajima, M., & Okadome, H. (2011). Effect of particle size of different crop starches and their flours on pasting properties. *Japan Journal of Food Engineering, 12*(1), 29–35. https://doi.org/10.11301/jsfe.12.29

Jin, Y., Li, J. Z., & Malaki Nik, A. (2018). Chapter 17-Starch-based microencapsulation A2-Sjöö, Malin. In L. Nilsson (Ed.), *Starch in food (Second edition)* (pp. 661–690). Woodhead Publishing.

Li, G., Wang, S., & Zhu, F. (2016). Physicochemical properties of quinoa starch. *Carbohydrate Polymers, 137*(Supplement C), 328–338. https://doi.org/10.1016/j.carbpol.2015.10.064

Liu, T. Y., Ma, Y., Yu, S. F., Shi, J., & Xue, S. (2011). The effect of ball milling treatment on structure and porosity of maize starch granule. *Innovative Food Science & Emerging Technologies, 12*(4), 586–593. https://doi.org/10.1016/j.ifset.2011.06.009

Loubes, M. A. (2015). *Dry and wet milling of rice in a planetary ball mill. milling kinetics, effect of milling conditions on flour and starch functional properties and mixture design of gluten free pasta*. Buenos Aires, Argentina: Industry Department, School of Exact and Natural Sciences, University of. Published PhD Thesis.

Loubes, M. A., Barrera, G. N., & Tolaba, M. P. (2016). High-impact wet-milling: Effects of steeping conditions on rice starch attributes. *Starch-Stärke, 68*(11–12), 1095–1102. https://doi.org/10.1002/star.201600092

Loubes, M. A., & Tolaba, M. P. (2014). Thermo-mechanical rice flour modification by planetary ball milling. *LWT-Food Science and Technology, 57*(1), 320–328. https://doi.org/10.1016/j.lwt.2013.12.048

Mizrahi, S. (2010). Syneresis in food gels and its implications for food quality. In L. H. Skibsted, J. Risbo, & M. L. Andersen (Eds.), *Chemical deterioration and physical instability of food and beverages* (pp. 324–348). Sawston: Woodhead Publishing.

Roa Acosta, D. F., Solanilla Duque, J. F., Agudelo Laverde, L. M., Villada Castillo, H. S., & Tolaba, M. P. (2020). Structural and thermal properties of the amaranth starch granule obtained by high-impact wet milling. *International Journal of Food Engineering*, (10), 16. https://doi.org/10.1515/ijfe-2020-0024

Roa, D. F., Baeza, R., & Tolaba, M. P. (2015). Effect of ball milling energy on rheological and thermal properties of amaranth flour. *Journal of Food Science and Technology, 52*(12), 8389–8394. https://doi.org/10.1007/s13197-015-1976-z

Roa, D. F., Santagapita, P. R., Buera, M. P., & Tolaba, M. P. (2014b). Ball milling of amaranth starch-enriched fraction. Changes on Particle size, starch crystallinity, and functionality as a function of milling energy. *Food and Bioprocess Technology, 7*(9), 2723–2731. https://doi.org/10.1007/s11947-014-1283-0

Roa, D. F., Santagapita, P. R., Buera, M. P., & Tolaba, M. P. (2014a). Amaranth milling strategies and fraction characterization by FT-IR. *Food and Bioprocess Technology, 7*(3), 711–718. https://doi.org/10.1007/s11947-013-1050-7

Sha, X. S., Xiang, Z. J., Bin, L., Jing, L., Bin, Z., Jiao, Y. J., et al. (2012). Preparation and physical characteristics of resistant starch (type 4) in acetylated Indica rice. *Food Chemistry, 134*(1), 149–154. https://doi.org/10.1016/j.foodchem.2012.02.081

Singh, N., Singh, J., Kaur, L., Singh Sodhi, N., & Singh Gill, B. (2003). Morphological, thermal and rheological properties of starches from different botanical sources. *Food Chemistry, 81*(2), 219–231. https://doi.org/10.1016/S0308-8146(02)00416-8

Steeneken, P. A. M. (1989). Rheological properties of aqueous suspensions of swollen starch granules. *Carbohydrate Polymers, 11*, 23–42.

Tan, X., Zhang, B., Chen, L., Li, X., Li, L., & Xie, F. (2015). Effect of planetary ball-milling on multi-scale structures and pasting properties of waxy and high-amylose cornstarches. *Innovative Food Science & Emerging Technologies, 30*, 198–207. https://doi.org/10.1016/j.ifset.2015.03.013

Wani, A. A., Singh, P., Shah, M. A., Schweiggert-Weisz, U., Gul, K., & Wani, I. A. (2012). Rice starch diversity: Effects on structural, morphological, thermal, and physicochemical properties-a review. *Comprehensive Reviews in Food Science and Food Safety, 11*(5), 417–436. https://doi.org/10.1111/j.1541-4337.2012.00193.x

Yang, W., Kong, X., Zheng, Y., Sun, W., Chen, S., Liu, D., et al. (2019). Controlled ultrasound treatments modify the morphology and physical properties of rice starch rather than the fine structure. *Ultrasonics Sonochemistry, 59*, Article 104709. https://doi.org/10.1016/j.ultsonch.2019.104709

Ye, J., Hu, X., Zhang, F., Fang, C., Liu, C., & Luo, S. (2016). Freeze-thaw stability of rice starch modified by improved extrusion cooking technology. *Carbohydrate Polymers, 151*, 113–118. https://doi.org/10.1016/j.carbpol.2016.05.026

Zhang, Z., Zhao, S., & Xiong, S. (2010). Morphology and physicochemical properties of mechanically activated rice starch. *Carbohydrate Polymers, 79*(2), 341–348. https://doi.org/10.1016/j.carbpol.2009.08.016